7th Scientific-Technical Conference Material Problems in Civil Engineering (MATBUD'2015)

Durability of air entrained cement mortars under combined sulphate and freeze-thaw attack

Wojciech Piasta[a],*, Julia Marczewska[a], Monika Jaworska[a]

*[a]Kielce University of Technology, Department of Civil Engineering and Architecture,
Al. Tysiąclecia Państwa Polskiego 7, 25-314, Kielce, Poland*

Abstract

The paper deals with experimental results of combined sulphate expansion and freeze-thaw attack on air entrained (AE) and non-air entrained (nAE) ordinary portland cement mortars. After prior freezing and thawing of the 4x4x16 cm mortar bars the part of them was subjected to sulphate attack of the 5% Na_2SO_4 solution. Another part of mortar bars was immersed in the sulphate solution for 110 days and then these bars were frozen and thawed. The resistance of nAE and AE mortars to regular sulphate and freeze-thaw attacks alone was tested as well. In order to compare damage degree of mortars in all environments, there were investigated long term linear strains (expansion), and compressive strength of mortars. Also the SEM and XRD analyses of mortars were carried out. Compared to the individual sulphate attack alone, prior freeze-thaw and following it sulphate attack affected significant acceleration of sulphate expansion of nAE and AE mortars as well, despite much better resistance of AE mortars to freezing and thawing. However, the prior sulphate attack significantly reduced AE mortars resistance to freezing and thawing. The SEM analysis showed that air voids in AE mortars were partially filled with ettringite. Its precipitation in air voids of AE mortars caused that the volume of air was diminished and freeze-thaw resistance of AE mortars was significantly decreased and it was as low as resistance of nAE mortars was. The complete destruction of AE mortars subjected to sulphate attack alone occurred earlier than that of nAE mortars did. Based on SEM analysis results it is suggested that lower sulphate resistance of AE mortars was due to higher porosity of the air void-paste interface and its higher initial w/c ratio compared to 'bulk paste' farther away from.

* Corresponding author. Tel.: +48 692-104-284;
  E-mail address: wpiasta@tu.kielce.pl

1. Introduction

When concrete is air entrained there occur some changes in microstructure of cement paste near the air void shell due to the presence of water-rich fresh paste containing significantly lower cement content. Air void-paste interfacial transition zone appears to be formed [1, 2]. Interfacial paste is of higher initial w/c ratio compared to bulk paste farther away from the interface. The width of the interface is around 15-30 μm from the air void surface [1,3]. In general it seems that the air void-paste interface is similar to aggregate-paste interfacial transition zone whose width is of 20–50 μm. Rashed and Williamson [2] have identified a distinct feature of air voids: a shell to the air void surface. The shell appears to be made up of small mineral particles and the thickness of the shell is 1–5 μm [1]. Ley et al. [4] found that the air-void shells consist of C–S–H with small amounts of ettringite needles on the surface of the void. The shell is denser than the paste which is directly adjacent to the shell. The ratio of calcium-to-silicon of the air-void shell was equal to about 1.1 [4] and this is lower than that of bulk cement paste C–S–H whose ratio amounts to 1.5 [5]. Moreover, no significant precipitation of portlandite occurs at the air void-paste interface, although the level of cement hydration around the pore is much higher [1]. This may probably have a positive influence on the sulphate resistance of the air entrained cement composites. Because concrete contains around 25–35% volume of cement paste and all of the air voids reside in the cement paste, a small percentage of air entrainment of concrete causes a significant change to the microstructure of the paste and to its pore structure in particular. Wong et al. [3] proved that air entrainment increases gaseous diffusivity and permeability by up to a factor of 2 at the air content 6% because the porosity near the air void boundary is about 2–3 times that of the bulk paste. This in turn suggests increased water permeability and easy access for the solution to the air entrained concrete. Due to freeze-thaw resistance it is significant that though air voids are permeable water absorption of AE concretes is not increased with increasing air content except when AE concretes are long term moisture cured. The solution transport in AE concrete is complex as it has a wide variety of pore structures. Therefore, the significant effect of air entrainment on sulphate expansion of AE concretes is probable.

According to Yu et al. [6] and Kunther et al. [7] expansion is related to the transformation of monosulphate crystals embedded in the C-S-H to ettringite. Initially incoming sulphate reacts with aluminate hydrates in large pores to give ettringite without expansion. After all this "freely available" aluminate has reacted, the concentration of sulphate ions in the pore solution increases by the rise of sulphate absorbed in C-S-H. In such a case, if monosulphate and gypsum are both present locally, the solution can be highly supersaturated with respect to ettringite, whose formation within C–S–H microstructure can then exert expansive forces due to crystallisation pressure arisen [8]. When the solution concentration reaches a critical level it provides the driving force for the precipitation of ettringite crystals in small pores within the C-S-H. In the case of AE mortars, Santhanam et al. [9] suggests that the entrained air voids provide sites for precipitation of the sulphate attack products. Thus, air voids might lead to a reduced damage in the paste. Although the space available for ettringite and gypsum is increased, according to Yu et al. [6] crystals that form in the air pore free space do not cause expansion because they can only form from "freely available" aluminate. The degradation starts when ettringite forms from the aluminate embedded in the C-S-H.

It is well established that adequate air entrainment with air voids of sufficient volume and fine size as well as close and regular spacing of the air voids excellently protects concrete against frost damage. There is some doubt as to whether the sulphate attack products and their precipitation in air pores will affect the subsequent frost resistance of properly air entrained cement composites. The effect of initial short-term action of frost on subsequent sulphate resistance is completely unknown. Also, the influence of air entrainment on the sulphate resistance of cement composites remains unexplained. In this context, it is necessary to perform direct tests to find out if the entrained air pores can improve the sulphate resistance, as suggested by Santhanam et al. [9] or have no effect, as driving forces for expansion are related to ettringite formed from monosulphate embedded in the C-S-H [6].

2. Experimental

2.1. Research objective and scope

The study aims to determine the effect of air entrainment on sulphate resistance, frost action and damage due to combined action of these two factors caused in cement mortars exposed to freezing and thawing, and sulphate attack of Na_2SO_4 solution. Since data in the literature are scarce, the attention was paid to clarifying the sulphate attack process after prior (initial) short-term frost action and to the frost action process in nAE and AE cement mortars after the initial sulphate attack.

Series of AE and nAE mortars were subjected to the following parallel degradation modes:

- sulphate attack in a 5% Na_2SO_4 solution alone
- freezing-thawing alone
- prior sulphate attack for 110 days → freezing-thawing
- 30 cycles of freezing-thawing → sulphate attack

The measurements of strains were carried out with the Graff-Kaufman's extensometer using 6 samples 40×40×160mm of each mortar per one exposure mode. The tests ended with the determination of the compressive strength of the mortars. The strength was also determined at the moment of the exposure conditions change, i.e. after 110 days of immersing the samples in the sodium sulphate solution and after 30 freeze-thaw cycles. The research programme included XRD and SEM analyses of mortars microstructure as well.

2.2. Materials

Mortars made from two different ordinary portland cements CEM I 42.5 R were studied. Chemical and phase compositions of the cement clinkers are shown in Tab.1. The w/c ratio was 0.60 with typical cement to sand 1:3 ratio. The samples were allowed to cure in water for 28 days. Half of the samples were air entrained with air entraining agent (surfactant from the class of alkyl sulphonates) in the amount of 0.2% by cement mass. The air content in the fresh mortars, determined in the pressure method, was 10 %± 1.

Table 1. Chemical and phase composition of cement clinker [%].

Cement	SiO_2	Al_2O_3	Fe_2O_3	CaO	$CaO_{(free)}$	MgO	SO_3	Cl-	Na_2O_{eq}	C_3S	C_2S	C_3A	C_4AF
CEM I „a"	19.5	6.0	3.1	62.1	1.75	1.7	2.6	0.03	0.8	67.0	6.49	10.9	9.32
CEM I „b"	21.31	5.01	3.36	65.06	1.53	1.95	0.74	0.03	0.79	71.0	9.19	5.12	11.45

3. Test results

The non air entrained mortar made from CEM I„b" immersed in the sodium sulphate solution for up to 170 days showed a slow uniform increase in expansion strains (Fig. 1a), followed by a rapid expansion within subsequent 60 days observed until the failure of the samples after 230 days. The AE and nAE mortars made from the same cement type disintegrated at similar strains (about 10‰), but the AE mortar exhibited much faster expansion leading to its complete destruction at 170 days. Compared to nAE mortars, the AE mortars made with CEM I„a" showed lower durability under sulphate conditions. After 140 days, the AE samples had a strain of 4.8‰ and were completely damaged (Fig. 1a). The nAE samples having reached an expansion of 5.15‰ disintegrated 30 days later, i.e., at 170 days. Note that in a 5% Na_2SO_4 solution, the AE samples made from both cement types were damaged earlier than the nAE mortar samples. During frost weathering the nAE mortar samples damaged earlier than the AE ones (Fig. 1b). The smallest strains of the samples after 80 freeze-thaw cycles were determined in the AE mortars made from CEM I„b" (0.16‰) and from CEM I„a" (0.4‰). After 80 cycles the strain of the nAE

mortar made from CEM I„b" was 3.5‰ and a complete destruction followed. The nAE mortar made from CEM I„a" had a strain of about 9‰ and failed as early as after 70 freeze-thaw cycles.
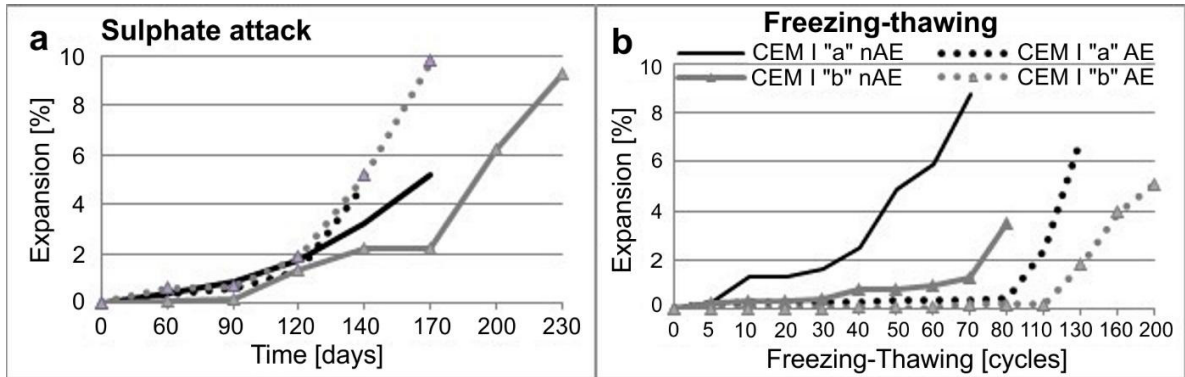

Fig. 1. Expansion of AE and nAE mortars samples a) immersed in the 5% Na_2SO_4 solution, b) frozen and thawed.

Expansion after the initial immersion in the sodium sulphate for 110 days did not exceed 2‰ (Fig. 2a). After the action of the Na_2SO_4 solution, the samples were subjected to freeze-thaw cycles which led to further increase in strain. Note that, regardless of differences in strain values, the failure of AE and nAE mortars made from individual cement took place after the same number of cycles. Also the frost resistance of the AE mortars, earlier exposed to the sulphate attack, decreased substantially and the number of cycles needed for damage was only 40-60, whereas under frost weathering (without sulphate attack) the failure took place after 130-200 cycles.

The AE mortars made from CEM I„a" after initial 30 freeze-thaw cycles and immersed in the sodium sulphate disintegrated as early as 60 days with strain of about 8‰ (Fig. 2b). Despite the high initial freeze-thaw durability, a rapid expansion was observed after 30 days immersion in the Na_2SO_4 solution. Note that when the samples made from the same cement were not frozen and thawed they were disintegrated after 170 days of sulphate attack. The nAE mortars made from CEM I„a" subjected to combined damaging action also had much lower durability than during the sulphate attack alone, and disintegrated after 90 days with the strain of 8.3‰. Both AE and nAE mortars made from CEM I„b" experienced no strain during the first freeze-thaw cycles. Following the immersion in the sodium sulphate, the samples of both mortars deteriorated after 120 days. At the moment of destruction, the nAE mortars had 5.2‰ strain, with 6.3‰ strain in the AE samples.
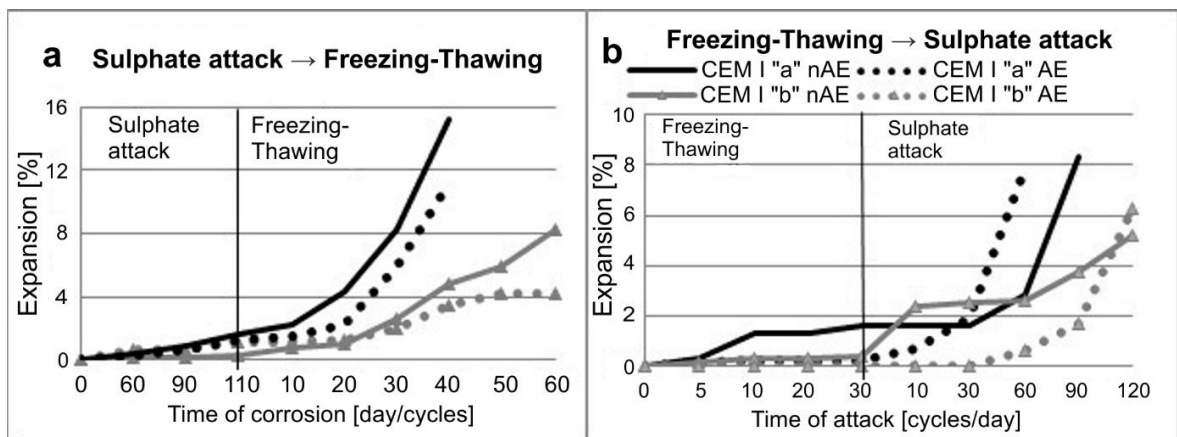

Fig. 2. Expansion of AE and nAE mortars sample a) immersed in the 5% Na_2SO_4 solution for 110 days and then frozen and thawed, b) frozen and thawed for 30 cycles and then immersed in the 5% Na_2SO_4 solution.

A joint interpretation of strength changes, expressed as a percentage of strength of 28-day cured individual mortar in Figs. 3 and 4 allows better comparison of their durability. Figure 3a shows the changes in strength for the AE and nAE mortars which were totally damaged due to freezing and thawing. Both AE and nAE mortar samples pre-immersed in the Na_2SO_4 solution and then subjected to freeze-thaw cycles disintegrated after the same number of cycles, i.e., after 60 cycles in the case of the cement CEM I,,b" mortars and 40 cycles in the case of the cement CEM I,,a" mortars. In both cases the decrease in strength was about 50-70%. As a result of freezing and thawing alone, the AE mortars made from cement CEM I,,b" showed about 20% decrease in strength after 200 cycles (Fig. 3b); the nAE mortars deteriorated as early as after 80 cycles. The strength of the nAE samples made from cement CEM I,,a" dropped by about 60% after 70 cycles, whereas the AE mortars survived 130 freeze-thaw cycles and prior to damage their strength decreased by about 50%.
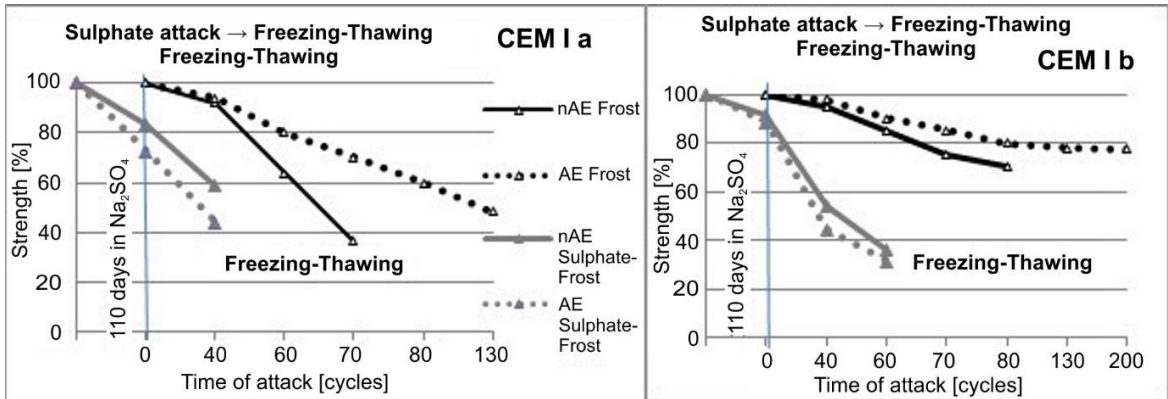

Fig. 3. Compressive strength of AE and nAE mortars damaged with freezing and thawing alone or damaged with prior sulphate attack and subsequent freezing and thawing a) cement CEM I,,a" mortar; b) cement CEM I,,b" mortar.
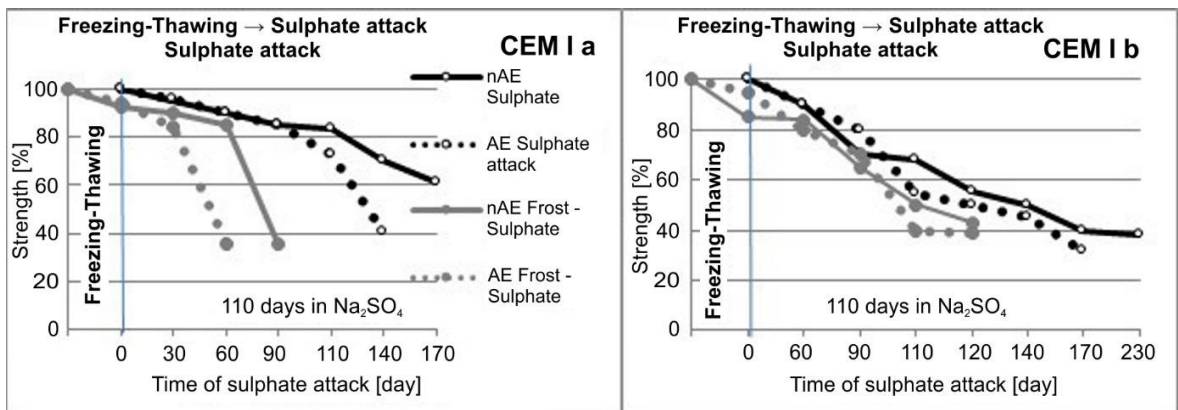

Fig. 4. Compressive strength of AE i nAE mortars damaged with sulphate attack alone or damaged with prior freezing and thawing and subsequent sulphate attack a) cement CEM I,,a" mortar; b) cement CEM I,,b" mortar.

Figure 4 shows percent strength of AE and nAE mortars made from both cements after the sulphate attack alone and after the sulphate attack preceded by freeze-thaw cycles. Compared to the nAE mortars, the air entrained ones subjected to sodium sulphate showed a bigger decrease in strength. In the case of the combined damaging action – first by 30 freeze-thaw cycles and then exposed to the sulphate attack, the decrease in strength of nAE and AE samples was similar.

The XRD analyses of AE and nAE mortars made of both cements indicate due to the sulphate attack a substantial amount of ettringite and gypsum was formed, likely with a greater amount of ettringite in the AE mortars. Smaller amount of portlandite occurs in the AE mortar. This suggests that sulphate attack is more advanced in these mortars. The SEM images of the fracture surfaces of mortar samples exposed to Na_2SO_4 action are shown in Fig. 5 a), b), c). The SEM analysis confirms the results from the XRD analysis and proves the presence of ettringite and gypsum in the microstructure. In both AE and nAE mortars, ettringite is the prevailing phase among products of sulphate attack. It precipitated mostly in air voids and capillary pores. Ettringite crystals were also found in the C-S-H compact microstructure, randomly embedded alone or in very small groups. In the AE mortar, ettringite crystals occurred in some air void to a varied extent. Several characteristic geometric arrangements of the ettringite crystals can be distinguished. It is noteworthy, however, that in each of these arrangements the crystals start growing from its end on the side of the inner surface of shell. One of such special arrangements, shown in Fig. 5a, is the radial arrangement in which ettringite needles lying along the radii of void grow until they fill it completely. Coarse air voids are often present, partially filled with radially arranged ettringite needles growing from the inner surface of shell, with the centre of the air void left empty. Small groups of needle-like crystals growing from the shell at single points in random directions (Fig. 5b) are another frequent arrangement of ettringite crystals inside air voids. Ettringite crystals passing through the microstructure of the shell into the air void (Fig. 5c) were also observed, but not frequently. Compared to the air voids, ettringite crystals embedded in the paste microstructure of the air void-paste interface were rarely observed. They were usually small and disorderly arranged.
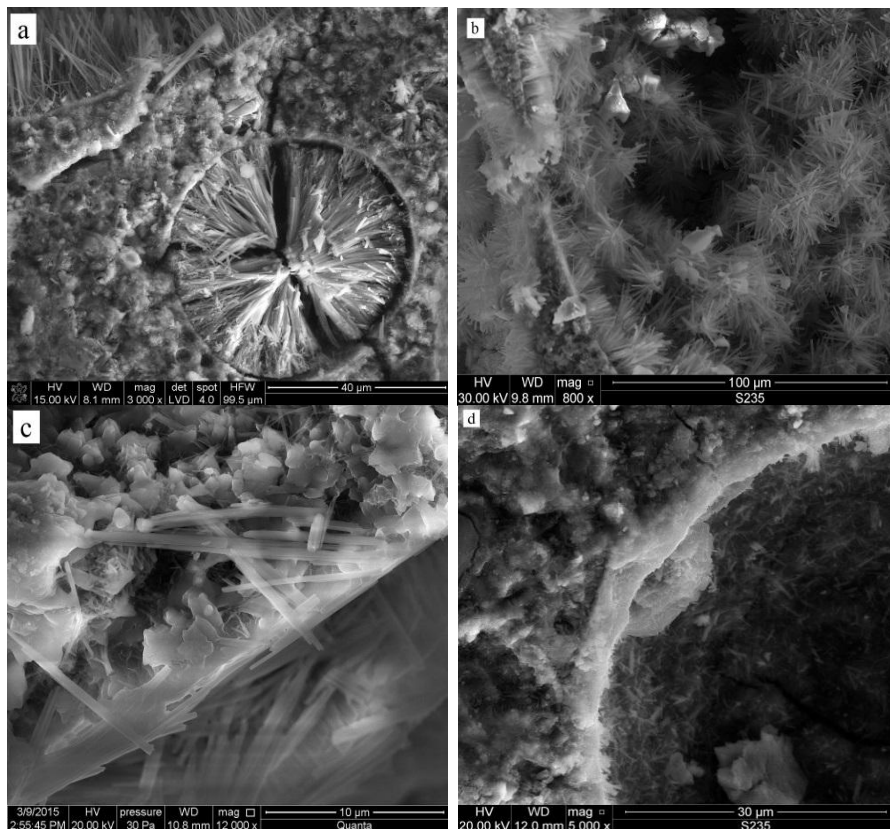

Fig.5. SEM images of the air entrained voids a) radial arrangement of ettringite in the void; b) needle-like ettringit crystals growing on the air void shell at single points in random directions; c) ettringite crystals passing through the microstructure of the shell into the air void; d) void shell and small ettringite crystals on the inner surface of the shell before sulphate attack.

4. Discussion

To explain the difference in the process of sulphate expansion of AE mortars, attention was paid to the microstructure of shells surrounding the air voids and adjacent paste in the mortars that have not been subjected to sulphate attack. The SEM image (Fig. 5d) shows that the shell has a clear edge from the side of the void and, in some cases, from the side of the paste. The phases passing from the interfacial paste to the void do not occur in the shell if no sulphate attack occurs. The microstructure of the air void shell is much denser compared to the adjacent paste, so pores were hardly observed in the microstructure of the shell. Limited quantities of fine ettringite needles are found to grow into the shell surface. Around the dense microstructure of the shell, the porous paste creates interface identified by Wong et al. [3] as the air void-paste interfacial transition zone. Note that no portlandite crystals adhering to the voids were observed on the SEM images. In the AE mortars exposed to sulphate attack, the ettringite formed mainly inside the air voids i.e. where small needles of ettringite had been formed before the sulphate attack started. The small crystals of ettringite formed as hydration product could act as the nucleation sources of the ettringite precipitated as the sulphate attack product. This nucleation, (Fig. 5d), is induced by very small ettringite crystals formed on the inner surface of the void shell.

Ettringite which was the product of sulphate attack, precipitated on the inner surface of the shell in different range and arrangements (Fig. 5c). Despite the tightness of the shells, indicated also by Ley et al. [4] relatively large quantities of ettringite were formed in voids, may be due to the large permeability of the air void-paste interfacial transition zone, and because of connections with the capillary pores causing the air voids are permeable [3]. Also, microcracks and local shell discontinuities may make access for sulphate solution easier. In the nAE mortars, the loosely arranged crystals occurred in the capillary pores. Also the sodium sulphate attack on the nAE mortars results in ettringite crystals precipitation disorderly embedding in the C-S-H phase. They are usually smaller than those occupying the air voids of the AE mortars. Decline in frost durability of the AE mortars subjected to prior sulphate attack was caused by ettringite filling some of the air void volume. Partially or fully filled air voids did not have enough free space to accommodate water pushed in by the ice forming during the freezing. Immersion of the AE mortars in the Na_2SO_4 solution for 110 days considerably reduced the durability of the AE mortars to the durability level of the nAE mortars under the same conditions. Another factor which accelerated frost damage of the AE mortars might be microcracks caused by sulphate expansion leading to lower strength levels.

Initial 30 cycles freezing-thawing of nAE mortars resulted in the significant acceleration of their sulphate expansion and ultimate damage.The AE samples did not show any significant strains or strength changes during 30 freeze-thaw cycles and their resistance to the subsequent sulphate attack was similar to that of the nAE samples, unlike during the sulphate attack alone when the AE samples exhibited much lower durability than the nAE mortar. In the case of the combined damage (freeze/thaw – sulphate attack), the acceleration of expansion and damage is most likely associated with increased permeability of mortars due to microcracks caused primarily in the nAE mortars by the freeze-thaw cycles. Observed in SEM images, the microstructure of mortars subjected to the combined destruction process was quite similar to that observed during an ordinary sulphate attack. Ettringite could be found in the air voids and the bulk paste. In the case of the combined deleterious process, however, microcracks in the paste were clearly visible. This may lead to the conclusion that accelerated ettringite formation was due to easy access made for the sulphate solution by the microcrackings resulting from earlier freezing and thawing.

5. Conclusions

1. In the Na_2SO_4 solution, AE cement mortars experienced faster expansion and damage than nAE mortars. The largest quantities of ettringite formed due to sulphate attack were observed in the air voids. This may result from the presence (before the sulphate attack) of very small crystals of ettringite acting subsequently as the nucleation source. It seems that accessibility of the air voids for the sulphate solution is most likely related to an existence of the porous and permeable air void-paste interfacial transition zone observed in SEM images.

2. In the nAE mortars, more resistant to the sulphate attack, expansion and ultimate destruction were accelerated substantially by prior freezing and thawing. In the case of the combined damage process, accelerated expansion and destruction might result from increased permeability of the mortars due to microcracks. Initial freeze–thaw affected sulphate expansion of AE mortars in much smaller degree.

3. The freeze-thaw resistance of AE mortars subjected to the initial sulphate attack was significantly lowered and comparable to that of the nAE mortars. The lowered frost resistance of the AE mortars subjected to prior sulphate attack was caused by filling the part of the air void volume with ettringite. The resistance to freezing and thawing of the nAE mortars initially subjected to Na_2SO_4 was reduced as well.

References

[1]   Corr DJ, Lebourgeois J, Monteiro PJM, Bastacky SJ, Gartner EM. Air void morphology in fresh cement pastes. *Cem Concr Res* 2002; 32:1025–31.
[2]   Rashed AI, Williamson RB. Microstructure of entrained air voids in concrete. *J Mater Res* 1991;6:2004–2012.
[3]   Wong HS, Pappas AM, Zimmerman RW, Buenfeld NR. Effect of entrained air voids on the microstructure and mass transport properties of concrete. *Cem Concr Res* 2011;41:1067–77.
[4]   Ley MT, Chancey R, Juenger M, Folliard KJ. The Physical and Chemical Characteristics of the Shell of Air-Entrained Bubbles in Cement Paste. *Cem Concr Res* 2009;39:417-25.
[5]   Diamond S. Cement Paste Microstructure An Overviewat Several Levels, Hydraulic Cement Pastes: Their Structure and Properties. *Cement and Concrete Association* 1976; p. 2–30.
[6]   Yu C,Sun W, Scrivener K. Mechanism of expansion of mortars immersed in sodium sulfate solutions. *Cem Concr Res* 2013;43:105–11.
[7]   Kunther W, Lothenbach B, Scrivener K. Influence of bicarbonate ions on the deterioration of mortar bars in sulfate solutions. *Cem Concr Res* 2013;46:23–9.
[8]   Scherer GW. Crystallization in pore. *Cem Concr Res* 1999;29:1347–58.
[9]   Santhanam M, Cohen MD, Olek J. Mechanism of sulfate attack: a fresh look Part 2. Proposed mechanisms. *Cem Concr Res* 2003;33:341–46.